

Influence of the Hydrophobic Phase on the Thermal Transitions of Water Sorbed in a Polymer Hydrogel Based on Interpenetration of a Hydrophilic and a Hydrophobic Network

M. Salmerón Sánchez,* G. Gallego Ferrer, M. Monleón Pradas, and J. L. Gómez Ribelles

Center for Biomaterials, Universidad Politécnica de Valencia, E-46071, Valencia, Spain

Received July 8, 2002; Revised Manuscript Received December 5, 2002

ABSTRACT: An interpenetrating polymer network with a low cross-linking content (so that phase separation appears) based on interpenetration of a hydrophobic, poly(ethyl acrylate), PEA, and a hydrophilic, poly(hydroxyethyl acrylate), PHEA, network is synthesized, swollen with different amounts of water, and subjected to cooling and heating scans in a differential scanning calorimeter. Results are compared with those of a pure hydrophilic network for the same water contents. Three qualitatively different kinds of thermograms are found in both cases, but in the case of the IPN, the hydrophobic component of the IPN significantly perturbs the melting process of water sorbed in the hydrophilic phase of the hydrogel. The hydrophobic component of the IPN has no appreciable influence on the specific (per unit hydrophilic component mass) water sorption, which remains almost the same as in the pure hydrophilic network, but it hinders the first-order transitions of water in the hydrogel and controls their temperature.

Introduction

A way of reinforcing a polymer hydrogel is through interpenetrating polymer networks (IPNs). IPNs are binary systems composed of two mixed polymers, each of which is individually cross-linked. If both polymers are not miscible and the cross-linking density is low, i.e., the number of monomer units between cross-links is high, then during the polymerization of the second network the growing chains will push apart the already existing chains of the first polymer, and a phase-separated IPN will be obtained. However, if the cross-linking density of the first network is high, the second network will grow interpenetrating the existing network and a homogeneous IPN can be obtained, achieving a forced compatibilization of the polymers.^{1,2}

Thermal transitions of water sorbed in polymer hydrogels are commonly related to the existence of different states of water in the hydrogel, including “bound” and “free” types of water in the polymer. Alternatively, the same phenomena can be explained as a consequence of the phase diagram of the system. Both approaches try to explain the existence of a certain amount of non-freezing water; the second one takes into account the increase of viscosity of the system as temperature is lowered, while the first one is focused on the polar interactions between water molecules and polymer chains.

For water molecules directly attached to polymer chains through hydrogen bonds the term “bound water” has been employed; for water molecules far away from, and not influenced by the polymer, the term “free water” is used.^{3–7} With this in mind, the existence of amounts of nonfreezable water in hydrogels has been explained by identifying the “bound water” with the nonfrozen water. The argument is almost evident: specific strong interactions of the water molecules with the polar groups of the polymer chains do not allow the migration of these molecules to the growing crystal phase. Thus,

a certain amount of water remains homogeneously mixed with the polymer chains, forming part of the hydrogel phase. However, the existence of nonfreezable water need not be explained by these interactions before taking into account other physical phenomena that occur while the temperature of the sample is lowered. In particular, there occurs a diffusion problem: as the system approaches the glass transition, the viscosity of the medium increases and water molecules cannot diffuse through the hydrogel phase; consequently, they cannot contribute to the continuous crystal growth and become “nonfreezable”.

That the polar interaction between water and polymer chains cannot be the sole factor responsible for the existence of amounts of “nonfreezable” water has been recently demonstrated: when a nonpolar solvent swells a hydrophobic network, the existence of noncrystallizable solvent is also found,⁸ and this cannot be explained invoking hydrogen-bonding interactions. The increasing viscosity of the swollen matrix as the system reaches temperatures close to the glass transition accounts for this behavior.

In this work we study the calorimetric behavior of sequential interpenetrating polymer networks with controllable degree of hydrophilicity, swollen with different amounts of water. In a previous work⁹ the thermal transitions of water in the pure homopolymer hydrogel of poly(hydroxyethyl acrylate), PHEA, were studied. In the present work we undertake a similar study in the IPN, poly(ethyl acrylate)–PHEA, systems. These polymer hydrogels have already been studied as regards their morphology, physical properties, water sorption, and water transport properties.^{10–12} These IPNs are phase-separated systems where hydrophilic and hydrophobic domains alternate. The size of these domains ranges from 30 to 100 nm; further, these microdomains are in turn composed of smaller domains ranging from 6 to 10 nm. The hydrophilic (hydrophobic) character of the microdomains is given by the larger proportion of hydrophilic (hydrophobic) nanodomains in

* Corresponding author: Tel +34-96-3877275; Fax +34-96-3877276, e-mail masalsan@fis.upv.es.

it. When swollen in water, the hydrophilic phase absorbs water as if the hydrophobic network were not present. The same result was found in poly(methyl acrylate)–PHEA IPNs.¹³ However, the present study reveals the importance of the surrounding medium on the thermal transitions of water in a hydrogel.

Material and Methods

Sequential interpenetrating polymer networks with different composition and constant cross-linker content were synthesized using 0.13 wt % of benzoin (Scharlau, 98% pure) as photoinitiator. A poly(ethyl acrylate), PEA (monomer from Aldrich, 99% pure), network was first polymerized with a 1 wt % of ethylene glycol dimethacrylate, EGDMA (Aldrich, 99% pure) as cross-linking agent. A sheet of around half-millimeter thickness was obtained. A pure poly(hydroxyethyl acrylate), PHEA, network was prepared in the same way. To form the IPNs, samples of the PEA network were swollen to equilibrium in mixtures of hydroxyethyl acrylate monomer with ethanol, containing 1% EGDMA and 0.13% of benzoin relative to monomer weight, with 20/80, 40/60, 60/40, and 80/20 weight ratios (weight of monomer/weight of ethanol). The swollen sample was exposed to ultraviolet light to polymerize the PHEA network. Low molecular weight substances were extracted from the IPN by boiling in ethanol for 24 h and then drying in vacuo to a constant weight. The weight fraction of the PHEA network in the IPNs, x_{PHEA} , was determined by weighing to be 0.37, 0.61, 0.73, and 0.78. Hereafter, IPNs with these PHEA compositions will be named as IPN1, IPN2, IPN3, and IPN4, respectively.

Samples for DSC were cut from the IPNs and the pure PHEA network plates and immersed in distilled water for different times to obtain hydrogels with different water contents, ranging from very low ones up to equilibrium values. Differential scanning calorimetry (DSC) was performed in a Pyris 1 apparatus (Perkin-Elmer). Helium gas was let through the DSC cell with a flow rate of 20 mL/min. The temperature of the equipment was calibrated by using cyclopentane and water. The melting heat of indium was used for calibrating the heat flow. The samples were subjected to a cooling scan from ambient temperature down to $-100\text{ }^{\circ}\text{C}$, followed by a heating scan from that temperature up to $20\text{ }^{\circ}\text{C}$, both scans at a rate of $10\text{ }^{\circ}\text{C}/\text{min}$.

The characteristic transition temperatures have been calculated from the DSC thermograms. For the glass transition of the swollen network, the temperature of the inflection point of the thermogram has been taken, whereas for the phase transition of water it is the temperature of the maximum of the large exothermal or endothermal peak that is taken.

The water content of the swollen gel was determined gravimetrically. The freezing amount of water was obtained by calculating the area of the crystallization peak in the DSC thermogram (enthalpy increment). The weight fraction of crystallizable water was calculated for each sample assuming a negligible heat of demixing of water in the polymer, the constancy of the melting heat of water with temperature, and that the specific melting heat of water in the gel is not different from that of pure water.

The water content in the swollen network is quantitatively given by the water weight fraction, ω , the ratio of the weight of water in the gel to the total weight of the swollen network:

$$\omega = \frac{m_{\text{water}}}{m_{\text{water}} + m_{\text{dry IPN}}} \quad (1)$$

The weight fraction of water sorbed per unit mass of PHEA in the IPN, ω' , will be also used, assuming that all water in the IPN belongs to the hydrophilic phase (PHEA):

$$\omega' = \frac{m_{\text{water}}}{m_{\text{water}} + m_{\text{dry IPN}} x_{\text{PHEA}}} \quad (2)$$

Note that for the pure hydrophilic network, PHEA, $\omega = \omega'$.

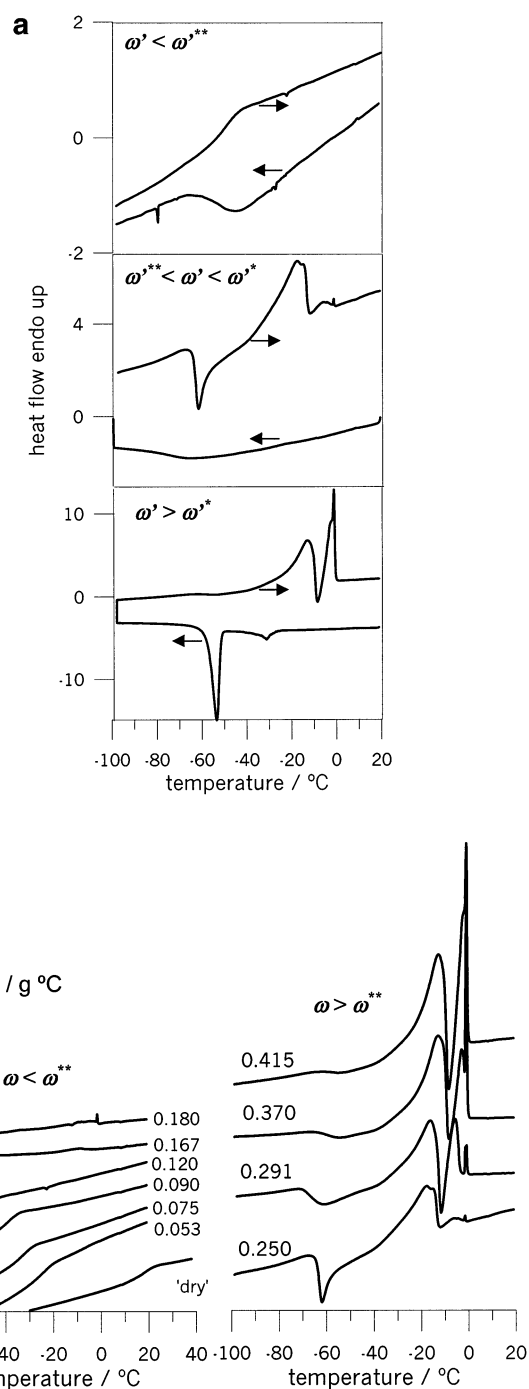


Figure 1. (a) Three qualitatively different kinds of thermograms, obtained after cooling (←) and heating (→) at $10\text{ }^{\circ}\text{C}/\text{min}$, for three different concentration ranges of water in the PHEA network. (b) DSC thermograms at a heating rate of $10\text{ }^{\circ}\text{C}/\text{min}$ for a PHEA network swollen with different contents of water (the weight fraction, ω , is indicated at each curve).

Results

Figure 1a shows three cooling and heating thermograms for the pure PHEA network that are representative of the qualitatively different kinds of thermograms for the samples (IPNs and pure PHEA) when swollen to different water concentrations. Two well-defined⁹ water contents ω'^* and ω''^* can be identified; the qualitatively different sets of thermograms are obtained according to whether the water content ω' of the gel falls below ω''^* , above ω'^* , or in between these two values. For the first range of compositions, $\omega' < \omega''^*$, only the

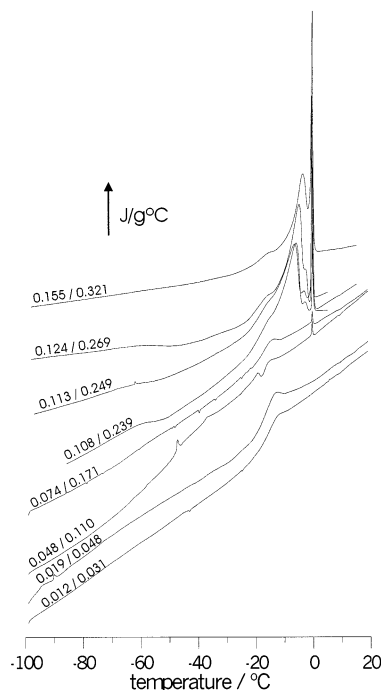


Figure 2. DSC thermograms at a heating rate of 10 °C/min for the IPN1 (PEA-i-PHEA, $x_{\text{PHEA}} = 0.37$) swollen with different contents of water (the weight fraction of water, ω , and the weight fraction per unit mass of PHEA in the IPN, ω' , are indicated at each curve).

glass transition of the swollen network appears on cooling without any sign of water crystallization. On heating the glass transition of the swollen gel is obtained in the same temperature interval, shifting toward lower temperatures as the water content increases with no sign of melting; all water is thus noncrystallizable. In the range of compositions $\omega'^{**} < \omega' < \omega'^*$, on cooling only the glass transition is observed, but on the subsequent heating scan three thermal phenomena are identified: the glass transition of the swollen network, crystallization on heating, and melting of the previously crystallized water. Finally, for water concentrations higher than ω'^* and up to equilibrium values water crystallizes on cooling, but now the glass transition is no longer visible; however, a change in the baseline can be identified. The heating thermogram shows an exotherm followed by a relatively complex melting zone. The glass transition is not visible on heating, but again a change in the baseline from the start to the end is appreciated. Figure 1b shows the heating thermograms for the pure PHEA network.

Figures 2–5 show the heating thermograms for the IPN1 to IPN4. The values of ω and ω' are indicated on each curve. Two separated glass transitions are visible on the xerogel thermograms (dry sample) of all IPNs, at the same temperature as those of the pure component networks.¹⁰ When IPN1 is swollen with different water concentrations, the glass transition temperature of the hydrophobic component (PEA) is constant and has almost the same value as in the pure PEA network. On the contrary, the hydrogel phase of the IPN shows the behavior described above; i.e., three qualitatively different thermograms can be identified depending on the water content of the material. The behavior of the PEA phase of the IPN is somewhat different for IPN2, IPN3, and IPN4: its glass transition also decreases when the water content of the IPN increases. Again the behavior

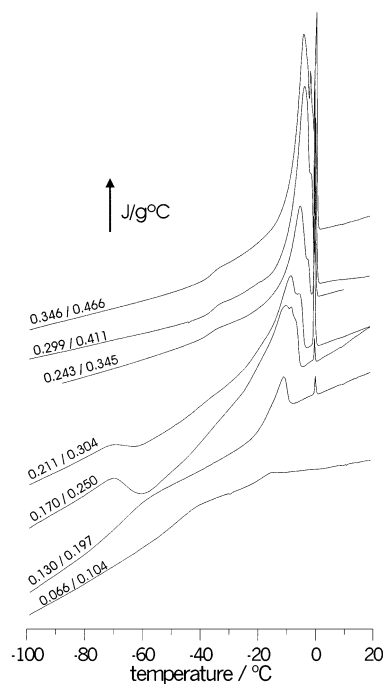


Figure 3. DSC thermograms at a heating rate of 10 °C/min for the IPN2 (PEA-i-PHEA, $x_{\text{PHEA}} = 0.61$) swollen with different contents of water (the weight fraction of water, ω , and the weight fraction per unit mass of PHEA in the IPN, ω' , are indicated at each curve).

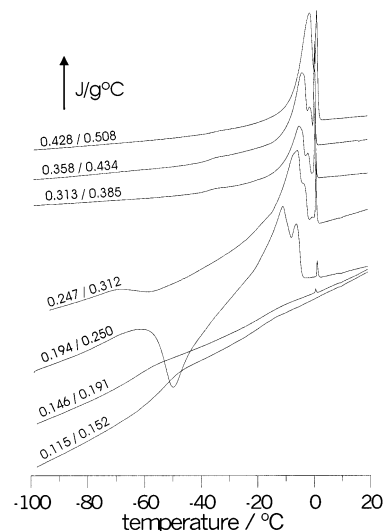


Figure 4. DSC thermograms at a heating rate of 10 °C/min for the IPN3 (PEA-i-PHEA, $x_{\text{PHEA}} = 0.73$) swollen with different contents of water (the weight fraction of water, ω , and the weight fraction per unit mass of PHEA in the IPN, ω' , are indicated at each curve).

of the hydrogel phase of the IPN is as expected, and different contents of water can be identified with the three qualitatively different thermograms described before. It is convenient to note that, for all IPNs, from a certain water concentration a narrow melting peak appears at 0 °C, which indicates the presence of a certain amount of phase-separated water that is not homogeneously mixed with the polymer hydrogel.

Discussion

Figure 6a represents the data obtained on pure PHEA from DSC thermograms (melting, crystallization, and glass transition temperatures) as a function of water

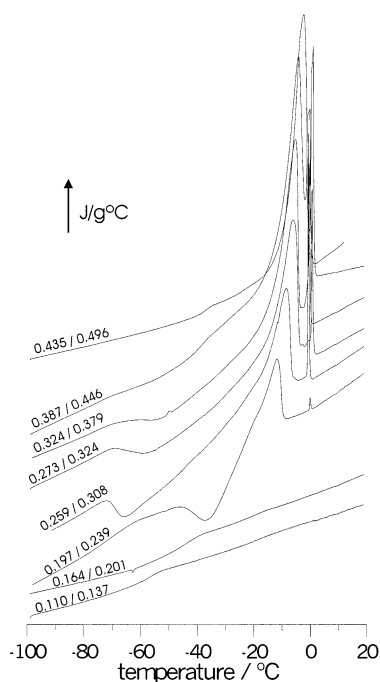


Figure 5. DSC thermograms at a heating rate of 10 °C/min for the IPN4 (PEA-i-PHEA, $x_{\text{PHEA}} = 0.78$) swollen with different contents of water (the weight fraction of water, ω , and the weight fraction per unit mass of PHEA in the IPN, ω' , are indicated at each curve).

content in a phase diagram. The melting temperature curve, T_m (the liquidus curve), shows the cryoscopic depression of the solvent in the hydrogel with respect to pure water melting temperature, i.e., 0 °C. The difference between T_m and the crystallization curve, T_c , is due to the supercooling needed to overcome the surface free energy barrier for the formation of the crystal phase. The glass transition temperature, T_g , of a binary system depends on composition and on both glass transition temperatures of the pure constituents.^{14,15} The three qualitatively different kinds of thermograms found experimentally can be assigned to three different intervals in the ω -axis of the phase diagram defined by the intersection of the T_g and T_m curves (ω'^*) and the intersection of the T_g and T_c curves (ω'^*). Simple inspection of the diagram or, alternatively, of the experimental DSC thermograms (Figure 1) suggests that $\omega'^* \approx 0.2$ and $\omega' \approx 0.3$; thus, water remains always homogeneously mixed with the hydrogel phase for compositions under 0.2; for compositions between 0.2 and 0.3 it does not crystallize on cooling but does so on heating, and for water contents from 0.3 on first-order transitions are present both on cooling and on heating.

The amount of nonfreezable water can be calculated through the experimentally measured enthalpy increments of the DSC thermograms.¹⁶ The mass of water that remains in the hydrogel after finishing the cooling scan turns out to be

$$m^*_{\text{water}} = m_{\text{wg}} - \frac{1}{\Delta H} \int_{\text{cooling}} \dot{Q}_{\text{exo}} dt \quad (3)$$

and after the cooling and subsequent heating scan

$$m^{**}_{\text{water}} = m_{\text{wg}} - \frac{1}{\Delta H} \left(\int_{\text{cooling}} \dot{Q}_{\text{exo}} dt + \int_{\text{heating}} \dot{Q}_{\text{exo}} dt \right) \quad (4)$$

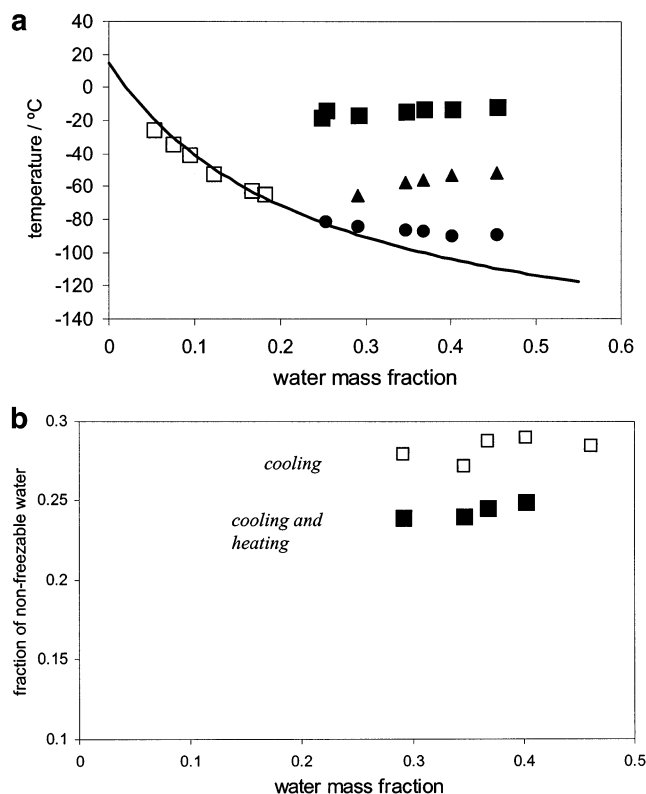


Figure 6. (a) Experimental temperature–composition diagram for the swollen pure PHEA network: (□) glass transition, (■) melting temperature, (▲) crystallization temperature of water on cooling. The solid line represents the prediction of the Couchman–Karasz equation with the parameters indicated in the text. (●) Predictions of the modified Couchman–Karasz equation. (b) Weight fraction of noncrystallizable water on cooling (□) and of noncrystallizable water on cooling and heating (■) vs the total weight fraction of water in the pure PHEA network.

In these equations m_{wg} is the water content of the IPN as determined gravimetrically, ΔH is the specific (per unit mass) melting heat of water, \dot{Q}_{exo} is the exothermic DSC heat flow, and t is time. The constancy of the amounts of nonfreezing water calculated from eqs 3 and 4 (Figure 6b) and the good agreement of the calculated values with those obtained through a direct inspection of the phase diagram or the thermograms (ω'^* , ω'^*) support the idea, already expressed in several works,^{8,16–18} that the phase diagram can explain the experimental thermograms observed for binary polymer–solvent systems.

Although our IPNs are phase-separated systems,¹⁰ when swollen in water, they show differences with respect to the pure hydrophilic PHEA network which can only be explained by a fine mixing in small regions of both the hydrophobic and the swollen hydrophilic material. In the water concentration range $\omega' < \omega'^*$ the T_g of the hydrogel phase of the IPNs superposes with that of the pure PHEA network (Figure 7), and all of them can be well described by the theoretical expression of Couchman–Karasz:¹⁴

$$T_g = \frac{(1 - \omega')\Delta c_{\text{pPHEA}} T_{\text{gPHEA}} + \omega' \Delta c_{\text{pwater}} T_{\text{gwater}}}{(1 - \omega')\Delta c_{\text{pPHEA}} + \omega' \Delta c_{\text{pwater}}} \quad (5)$$

In this equation $T_{\text{gwater}} = 134$ K and $\Delta c_{\text{pwater}} = 1.94$ J/(g K) have been taken from ref 19, while the values for PHEA ($T_{\text{gPHEA}} = 287$ K, $\Delta c_{\text{pPHEA}} = 0.38$ J/(g K)) have

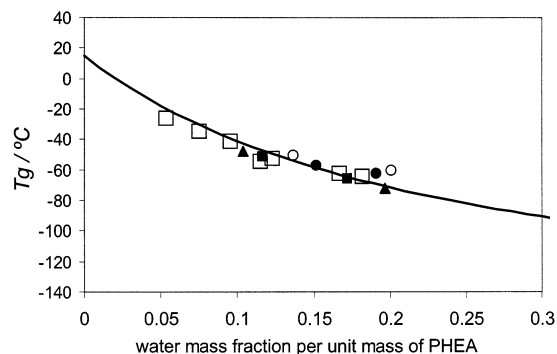


Figure 7. Evolution of the glass transition of the PHEA phase as a function of the water content per unit mass of the PHEA phase in the IPN: (□) pure PHEA network, (■) $x_{\text{PHEA}} = 0.37$, (▲) $x_{\text{PHEA}} = 0.61$, (●) $x_{\text{PHEA}} = 0.73$, (○) $x_{\text{PHEA}} = 0.78$.

been obtained experimentally by us. This fact suggests that practically all water sorbed by the IPN in this range is homogeneously mixed in the hydrophilic phase with the PHEA chains, and the PEA network remains “dry”. By contrast, a decrease of almost 20 °C is observed in the glass transition of the PEA phase in IPNs with PHEA content higher than 40% for high water contents. This finding can be also explained with eq 5 but for the PEA phase in the IPN: water contents in the PEA phase of only 0.05 (mass fraction of water per unit mass of PEA in the IPN) produce such a large decrease in the glass transition temperature because of the high slope of the Couchman–Karasz curve.

At water contents higher than ω'^{**} the glass transition temperature of the hydrophilic phase is no longer seen in the thermograms because the exothermic first-order transition overlaps with the glass transition step. A way of estimating the position of these “invisible” T_g under the crystallization exotherms is still eq 5, but for values of the hydrogel compositions modified in a way such as to detract the amount of water which has crystallized and is no longer mixed with the polymer.²⁰ The constancy of the T_g values thus determined (Figure 6a) is a further support of the glass transition as the factor that determines the amount of water that cannot crystallize.

An inspection of the DSC thermograms for the IPNs (Figures 2–5) seems to suggest that melting of water crystals does not take place before the hydrophobic component has passed its glass transition. Figure 8 shows two thermograms corresponding to the pure PHEA network and the IPN1, with approximately the same water content per unit mass of the hydrophilic component ($\omega' = 0.25$ in both cases). On heating, water starts to freeze at around -70 °C, after the glass-to-rubber transition in PHEA allows it, but the phenomenology of these transitions is significantly different. The pure PHEA network shows a narrow exotherm followed by a melting endotherm that can be inferred to start around -40 °C, taking into account the change of slope in the baseline. On the contrary, in IPN1 water crystallizes on heating along a wide and smooth exotherm (from -70 to -20 °C approximately) and melts in the IPN at temperatures higher than in the pure PHEA. Thermodynamic considerations show that water homogeneously mixed with a pure hydrogel can freeze on heating between the temperatures $T_g(\omega'^*)$ and $T_g(\omega'^{**})$.¹⁶ The results now presented suggest that this is not the case when the hydrophilic phase is completely surrounded by a hydrophobic component: the melting

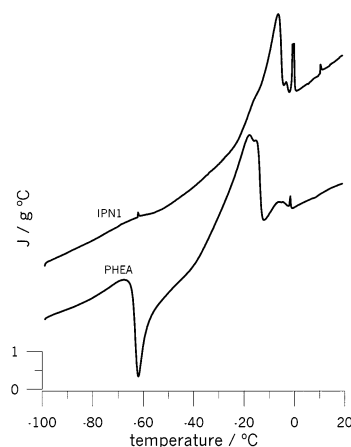


Figure 8. DSC thermograms for the pure PHEA network and IPN1 (PEA-i-PHEA, $x_{\text{PHEA}} = 0.37$) with the same water content per unit mass of PHEA ($\omega' = 0.25$).

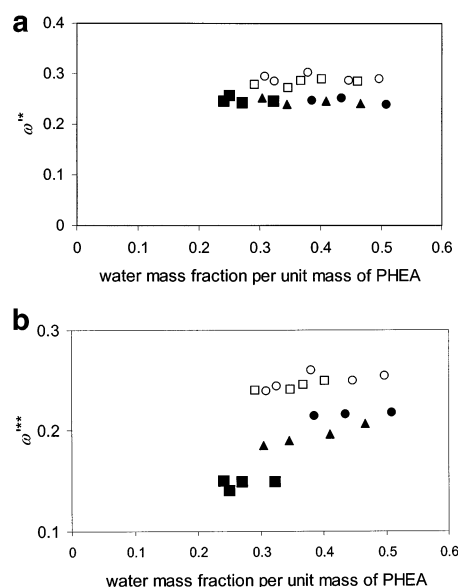


Figure 9. (a) Weight fraction of noncrystallizable water on cooling, ω'^* , vs water content per unit mass of PHEA in the IPN and (b) weight fraction of noncrystallizable water on cooling plus heating, ω'^{**} , vs water content per unit mass of PHEA in the IPN: (□) pure PHEA network, (■) $x_{\text{PHEA}} = 0.37$, (▲) $x_{\text{PHEA}} = 0.61$, (●) $x_{\text{PHEA}} = 0.73$, (○) $x_{\text{PHEA}} = 0.78$.

of water somehow is prevented by the surrounding PEA phase. This fact is found also in IPNs 2–4, but in these cases the glass transition of the PEA phase takes place at lower temperatures, according to the prediction of the Couchman–Karasz equation. The composition of the PHEA phase when crystallization on cooling has finished, ω'^* , is almost the same for all IPNs and similar to that of pure PHEA (Figure 9a). The situation changes when ω'^{**} is considered: Figure 9b shows a continuous increase in ω'^{**} as the concentration of the hydrophilic component of the IPN is increased. Since this influence of the hydrophobic component of the IPN on the melting of water depends on the hydrophilic degree of the xerogel, it is suggested that this phenomenon might be a consequence of the morphology of the material: these IPNs are phase-separated systems in which two types of microdomains alternate, one preferentially of hydrophilic nature and the other preferentially of hydrophobic nature. The microphases are composed of smaller nanodomains as revealed by the transmission electron micrographs.¹⁰ Co-continuity of the hydrophilic and the

hydrophobic phases in the IPNs is present from a concentration of the hydrophilic component in the IPN higher than 40%. The results obtained in this work suggest that the "degree" of this co-continuity increases as the PHEA content in the IPN increases. In IPN1 the glass transition of the PEA phase does not depend on the water content of the hydrogel and remains the same as that of the dry PEA homopolymer (Figure 2). In IPNs 2–4, with co-continuous PHEA phase, the hydrophobic phase is also plasticized by water, the glass transition temperature of the PEA phase in the swollen hydrogels decreases as the PHEA content in them increases, and the ω'^{**} value increases with PHEA content of the IPN.

The physical picture which explains these findings is not at all intuitive at first sight. If we consider a cooling-plus-heating cycle of the hydrogels, the following processes can be thought to occur. As temperature is lowered, the first transition to take place is the PEA glass transition. Water is at these temperatures homogeneously mixed with the polymer of the hydrophilic phase, PHEA, which is in the rubbery state. As the temperature decreases further, water starts segregating from the PHEA phase and crystallizes. This phase separation of water from the gel phase is arrested by the increase of viscosity of the medium when the gel attains its glass transition as temperature is further lowered. From that temperature on, the vitreous gel thus retains some amount of water that has remained mixed with the polymer and nonfrozen. Since now the phases present in the system are either crystalline (the pure water segregated) or vitreous (the hydrophobic PEA phase and the gel PHEA–water phase), nothing else happens (in the experimentally accessible time scale) while the cooling stage comes to an end.

During the subsequent heating stage, the first phenomenon to occur is the glass transition of the PHEA gel phase. From that temperature on the gel phase is again in the rubbery state, and water can again separate from it and grow the crystalline phase while crystallization is still thermodynamically favored, i.e., while $T < T_g(\omega'^{**})$. Up to this point the experimental behavior fully agrees with the just described account of the facts derived from phase diagram considerations, as happens in homogeneous hydrogels. In homogeneous hydrogels water that had phase-separated and crystallized either on cooling or on heating starts melting immediately above $T_g(\omega'^{**})$ as the temperature continues to rise. By contrast, in the heterogeneous hydrogels of the present work water does not melt immediately above $T_g(\omega'^{**})$, and only after the temperature of the system surpasses the glass transition temperature of the hydrophobic PEA phase does the melting of water start.

This anomalous melting behavior of water in the IPNs cannot be a consequence of the growth of water crystals under pressure: thermodynamic considerations show that an increase in pressure would lead not to an increase but to a decrease in the transition temperature, since the specific volume of ice is higher than that of liquid water. If the water crystals grow in the gel phase, keeping the equilibrium with it, then their melting temperature should be given, using the Flory–Huggins theory,²¹ by

$$\frac{1}{T_m} - \frac{1}{T_m^0} = \frac{-R}{\Delta H_f} \{ \ln(1 - \phi_{\text{polymer}}) + \phi_{\text{polymer}} + \chi \phi_{\text{polymer}}^2 \} \quad (6)$$

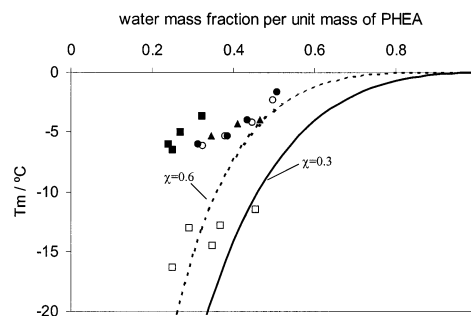


Figure 10. Evolution of the melting temperature of water in polymer IPNs: (□) pure PHEA network, (■) $x_{\text{PHEA}} = 0.37$, (▲) $x_{\text{PHEA}} = 0.61$, (●) $x_{\text{PHEA}} = 0.73$, (○) $x_{\text{PHEA}} = 0.78$. The solid lines represent the prediction of the Flory–Huggins relation for two values of the interaction parameter.

where ΔH_f is the melting heat of water, R is the universal gas constant, ϕ_{polymer} is the volume fraction of the polymer in the gel, and χ is the polymer–solvent interaction parameter. Figure 10 shows the experimental melting temperatures and the prediction of eq 6 for different values of the χ parameter. The experimental melting points of water in IPNs (Figure 10) are above any reasonable curve predicted by the Flory–Huggins theory if χ is the interaction parameter of water and PHEA. However, if the water crystals are not formed in the bulk phase of the hydrophilic component of the IPN, their melting temperature is no longer determined by the equilibrium condition with the hydrogel phase. Equilibrium can be established between both phases only if the melting water can rapidly diffuse into the gel phase. If the crystal has grown at the interface, however, it limits alongside one of its faces with the hydrophobic phase, which moreover is in the vitreous state. Melting of water is likely to start precisely along this interface, where defects and heterogeneities in the crystal structure are more likely to occur. This water cannot diffuse into the hydrophilic phase at a sufficient rate to maintain equilibrium, which would correspond to the liquidus curve predicted by eq 6; its melting temperature is thus that of a pure bulk water phase (0 °C) diminished by the temperature drop caused by size effects according to the Gibbs–Thomson formula

$$T_m - T_m(d) = \frac{4\sigma T_m}{\Delta H_f \rho d} \quad (7)$$

in which $T_m(d)$ is the melting point of crystals of size d , ρ is the density of solid water, and σ is the surface energy of the solid–liquid interface. If it is assumed that $4\sigma/\Delta H_f$ takes the same value in our system as does for almost all metals²³ and for several polymer monocrystals,²⁴ the Gibbs–Thomson relation would predict a melting point depression around 1–5 °C for crystal sizes between 50 and 10 nm. This crystal size has been found also in water ice in a poly(vinyl alcohol) hydrogel.²⁵ These values would explain the experimental melting temperature of water in the heterogeneous systems (Figure 10) as a depression with respect to the melting temperature of pure bulk water, 0 °C, and indirectly support the idea that crystalline water is formed at the interface between the hydrophilic and the hydrophobic networks.

The hydrophobic PEA phase surrounds ice crystals that have been formed at the interface and hinders

diffusion of water molecules from the crystal to the hydrogel.

Conclusions

Thermal transitions of water in hydrogels are complex phenomena that have to be explained taking into account the whole environment that surrounds water molecules. Melting and crystallization of water in a homogeneous hydrogel can be explained in the simple thermodynamic framework of the phase diagram of the system. However, in the system studied in this work, a phase-separated interpenetrated polymer network formed by a hydrophilic and a hydrophobic component, the influence of the hydrophobic component on the thermal transitions of water has a marked and unexpected effect.

Water can be considered to be in the hydrophilic phase of the IPN, whereas the hydrophobic component remains "dry". The effect of water is to lower the glass transition temperature of the PHEA phase in the IPN following the same pattern as in the case of a pure hydrophilic network. However, from a certain water concentration on the first-order transitions cease to correspond to equilibrium conditions, because ice crystals are formed at the interface and the hydrophobic phase prevents the diffusion of liquid water to the hydrophilic phase as melting proceeds. The experimental fact is that water melts at higher temperatures than predicted by the thermodynamic equilibrium between crystal water and the hydrogel phase. The melting temperature of water can be explained by the size effects of the phase formed accounted for by the Gibbs–Thomson equation.

Acknowledgment. Authors acknowledge the support of CICYT through the MAT99-0509 project.

References and Notes

- (1) Salmerón Sánchez, M.; Gallego Ferrer, G.; Torregrosa Cabanilles, C.; Meseguer Dueñas, J. M.; Monleón Pradas, M.; Gómez Ribelles, J. L. *Polymer* **2001**, *42*, 10071–10075.

- (2) Li, B. Y.; Bi, X. P.; Zhang, D. H.; Wang, F. S. In *Advances in Interpenetrating Polymer Networks*; Kempler, D., Frisch, K. C., Eds.; Technomic: Lancaster, 1994.
- (3) Corkhill, P. H.; Jolly, A. M.; Ng, C. O.; Tighe, B. J. *Polymer* **1987**, *28*, 1758–1766.
- (4) Barnes, A.; Corkhill, P. H.; Tighe, B. J. *Polymer* **1988**, *29*, 2191–2202.
- (5) Hofer, K.; Mayer, E.; Johari, G. P. *J. Phys. Chem.* **1990**, *94*, 2689–2696.
- (6) Smyth, G.; Quinn, F. X.; McBrierty, V. J. *Macromolecules* **1988**, *21*, 3198–3204.
- (7) Ishikiriyama, K.; Todoki, M. *J. Polym. Sci., Part B: Polym. Phys.* **1995**, *33*, 791–800.
- (8) Salmerón Sánchez, M.; Monleón Pradas, M.; Gómez Ribelles, J. L. *J. Non-Cryst. Solids* **2002**, *307–310*, 750–757.
- (9) Kyritsis, A.; Pissis, P.; Gómez Ribelles, J. L.; Monleón Pradas, M. *J. Non-Cryst. Solids* **1994**, *172–174*, 1041–1046.
- (10) Gallego Ferrer, G. Dr. Eng. Sci. Thesis, Universidad Politécnica Valencia, 2001.
- (11) Gallego Ferrer, G.; Monleón Pradas, M.; Gómez Ribelles, J. L. Results to be published.
- (12) Gallego Ferrer, G.; Monleón Pradas, M.; Gómez Ribelles, J. L.; Pissis, P. *J. Non-Cryst. Solids* **1998**, *235–237*, 692–696.
- (13) Gómez Ribelles, J. L.; Monleón Pradas, M.; Gallego Ferrer, G.; Peidro Torres, N.; Pérez Giménez, V.; Pissis, P.; Kyritsis, A. *J. Polym. Sci., Part B: Polym. Phys.* **1999**, *37*, 1587–1599.
- (14) Couchman, P. R. *Macromolecules* **1978**, *11*, 1156–1164.
- (15) Gordon, M.; Taylor, J. S. *J. Appl. Chem.* **1952**, *2*, 493–498.
- (16) Rault, J.; Lucas, A.; Neffati, R.; Monleón Pradas, M. *Macromolecules* **1997**, *30*, 7866–7873.
- (17) Rault, J.; Ping, Z. H.; Nguyen, Q. T. *J. Non-Cryst. Solids* **1994**, *172–174*, 733–736.
- (18) Franks, F. In *Thermal Analysis*; Hemminger, W., Ed.; Birkhaeuser: Basel, Switzerland, 1980; Vol. 2.
- (19) Johari, G. P.; Hallbrucker, A.; Mayer, E. *Nature (London)* **1987**, *330*, 552–553.
- (20) Hodge, R. M.; Edward, G. H.; Simon, G. P. *Polymer* **1996**, *37*, 1371–1376.
- (21) Flory, P. J. In *Principles of Polymer Chemistry*; Cornell University Press: Ithaca, NY, 1953.
- (22) Defay, R.; Prigogine, I. In *Surface Tension and Adsorption*; John Wiley & Sons: New York, 1966.
- (23) Wautelet, M. J. *J. Appl. Phys.* **1991**, *24*, 343–346.
- (24) Elias, H. G. In *Macromolecules*; Plenum Press: New York, 1977.
- (25) Dowell, L. G.; Rinfret, A. P. *Nature (London)* **1960**, *188*, 1144–1149.

MA021069P